

# Synthesis and Characterization of ZnO Nanoparticles using *Moringa Oleifera* Leaf Extract: Investigation of Photocatalytic and Antibacterial Activity

Sukanta Pal<sup>1</sup>, Sourav Mondal<sup>1</sup>, Jayanta Maity<sup>1,\*</sup> and Ratul Mukherjee<sup>2</sup>

<sup>1</sup>Department of Chemistry, Sidho-Kanho-Birsha University, Purulia, 723104, West Bengal, India.

<sup>2</sup>Department of Microbiology, J.K. College, Purulia, 723101, West Bengal, India.

(\* Corresponding author: jayantaptrl@gmail.com

(Received: 25 August 2017 and Accepted: 02 December 2017)

## Abstract

In this paper, we report the synthesis of ZnO nanoparticles using *Moringa Oleifera* (Drumstick) leaves as natural precursor via precipitation method. Formation and characterization of ZnO nanoparticles was established by UV-VIS spectroscopy, Fourier transform infrared spectroscopy, scanning electron microscopy and X-ray diffraction. The synthesized nanoparticles have hexagonal wurtzite structure of an average grain size of 52 nm confirmed from X-ray diffraction analysis. The synthesized ZnO nanoparticles have been employed as photocatalytic agent to degrade the organic dye viz. Titan yellow under visible light by exposing the visible light for one hour. ZnO nanoparticles degraded almost 96% of titan yellow dye. We also studied the antibacterial activity and it was found that the synthesized ZnO nanoparticles have potential applications in antibacterial activity. For antibacterial studies we used *Bacillus subtilis* as a gram positive and *Escherichia coli* as gram negative bacteria.

**Keywords:** ZnO nanoparticles, Photocatalytic degradation, Antibacterial activity.

## 1. INTRODUCTION

In modern research era of any branch of science, nanotechnology has found enormous interest. Nanoparticles (NPs) play an essential role as building blocks of nanotechnology. Nowadays, nanoscience as well as nanotechnology is widely applied in different fields mainly in sensor, electronic, antibacterial, water purification, cosmetic, biomedical, pharmaceutical, environmental, catalytic and material applications. The size, crystallinity and morphology of the nonmaterial can greatly influence their catalytic, magnetic, electronic and optical properties [1]. The main advantages of nanoparticles synthesis at room temperature and from plant extracts are partly fulfill the green synthesis [2]. The metal and metal oxide nanoparticles are synthesized by physical, biological, chemical and very recent green approaches. Recently, green synthesis has become popular way to

synthesize NPs due to its low cost, environment compatibility, synthesizable in ambient atmosphere and non-toxicity [3]. The noticeable importance of Zinc oxide and ZnONPs is found as very good semiconductor in nature with wide range of band gap (3.37) having room temperature dependent high excitation binding energy (60 meV) [4]. Zinc oxide and ZnONPs have excellent thermal and chemical stability with exceptional optical behavior [5]. Now a day the considerable interest was seen in biosynthesis of different nanoparticles as well as photo degradation properties. Recently different metal and metal oxide nanoparticles were reported for their efficient photo degradation effect in presence of visible light illumination [6]. Since, different plant extracts are the main source of large scale synthesis of NPs via green way which includes the synthesis of

several noble metal nanoparticles like Au, Ag and Pd. For this extracts from different plant organs e.g. geranium leaves, lemongrass, neem leaves, aloe-vera and others have been reported [7, 8, 9, 10, 11]. Moreover the important applications of ZnONPs towards environmental and biological fields are like drug delivery, biological sensing, biological labeling, gene delivery and nano medicine are reported [12, 13, 14, 15]. ZnONPs also have artificial protected applications for antibacterial, anti-diabetic, antifungal, acaricidal, pre-diculicidal, larvicidal activities [16, 17, 18, 19, 20]. Different medicinal plant and their leaf and calyx extract are found to have important properties such as diuretic, antioxidant, blood pressure suppressive, chemo-protective, hypotensive, anti-tumor and anti-cancerous effect [21, 22, 23, 24, 25]. Various organic color dyes were applied to the textile industry, during dye fabrication of textile a large amount of wastewater containing toxic and colored dyestuff have led to the severe surface water and ground water contamination. Such toxic pollutants usually removed by various physical and chemical methods, such as electrocoagulation [26], coagulation / flocculation [27] and coagulation/carbon adsorption process [28]. Karunakaran *et al.* [29] showed the antimicrobial properties of ZnONPs towards both gram positive and gram negative bacteria. Mahdiyeh *et al.* [30] synthesized ZnO nanowires via hydro-thermal process at 90 °C from zinc acetate dihydrate. Moj *et al.* [31] have bio-synthesized silver nanoparticles using Mine Soil Bacteria as natural precursor that showed antibacterial activity.

In our present work we have synthesized ZnONPs by using *Moringa Oleifera* (Drumstick) leaves as natural precursor. The dimension of prepared nanoparticles was about 52 nm and different techniques used for its characterization. We also studied the photocatalytic activity of synthesized ZnO nanoparticles to degrade the organic dye titan yellow as a representative dye and antibacterial activity

against gram positive and gram negative bacteria.

## 2. EXPERIMENTAL

### 2.1. Collection of Sample

Fresh *Moringa Oleifera* leaves were collected from university campus. Leaves were washed thoroughly by water and were allowed to dry in air at room temperature.

### 2.2. Chemicals, Solvents and Starting Materials

Zinc acetate dihydrate, ammonium carbonate, sodium hydroxide pellets and other chemicals were purchased from Merck (India) Ltd. All chemicals were used without further purification.

### 2.3. Preparation of Moringa Oleifera Leaf Extract

5 grams of *Moringa Oleifera* leaves were washed thoroughly with distilled water and both surface of leaves were sterilized using alcohol by gentle rubbing. These leaves were heated for 40 min in 100 ml of distilled water at 50°C. Then the extract was filtered with Whatman 41 filter paper. The filtrate was stored in a cool and dry place.

### 2.4. Synthesis of Zinc Oxide Nanoparticles

For the synthesis of zinc oxide nanoparticles by precipitation reaction process, 10 ml of *Moringa Oleifera* leaf extract was mixed with 50 ml 20% NaOH solution. Then 5 ml solutions of that mixture and 50 ml distilled water were taken in a 250 ml beaker and kept stirring for 1 h. Then zinc acetate (2.1g in 100ml water), ammonium carbonate (0.96g in 100ml) solutions were added drop wise into the beaker simultaneously with constant stirring. After the completion of reaction, the suspension was kept stirring at 750 rpm for 1h at 24°C temperature. Finally, precipitate was filtered, washed with ammonia solution followed by ethanol for several times. Then the precipitates were dried under vacuum for 12 hours and calcinated in a hot air oven at 350°C for 5

hours [Figure 1]. Then zinc oxide nanoparticles were collected and stored in vacuum for further use.

## 2.5. Physicochemical Characterization of ZnO Nanoparticles

The synthesized ZnO-NPs were characterized by UV–visible spectrophotometer (Perkin Elmer Lambda 35) at wavelength of 350–500 nm. The chemical composition and the functional groups present in the synthesized ZnONPs were studied by using Perkin Elmer (LI60300 spectrum two Lita SN 96499) FTIR-ATR spectrometer using KBr pellet in the range of 4000–400 $\text{cm}^{-1}$ . The size and morphology of the synthesized ZnONPs were characterized by X-ray diffraction (XRD) pattern and Scanning Electron Microscopy (SEM). The XRD pattern was measured by X-ray diffraction analyzer Benchtop PROTO AXRD with CuK $\alpha$  target and Ni- filter in the range of 10 to 80. The SEM images were obtained by using Scanning Electron Microscope at voltage 15 KV (Model no-JEOL JSM 5800).

## 2.6. Photocatalytic Activity of ZnONPs under Visible Light

The photo-catalytic degradation activity of titan yellow dye solution was evaluated by the synthesized ZnONPs. All the experiments were performed in the presence of sun light. Prior to the experiment, a suspension was arranged by adding 100 mg of synthesized ZnONPs and 100 ml of titan yellow dye solution ( $1.2 \times 10^{-4}$  M) in a 250 ml beaker placed on a magnetic stirrer at sunlight. Later, the mixture solution was kept in the dark for 10 min to set up the adsorption equilibrium. 5 ml reaction mixtures were taken at regular time interval (10 min) and centrifuged the solution for measurement. The absorption spectrum of the suspension mixture was measured periodically using an UV–visible spectrophotometer.

The percentage of dye degradation was calculated using the following formula:

## Synthesis of ZnONPs and Dye degradation

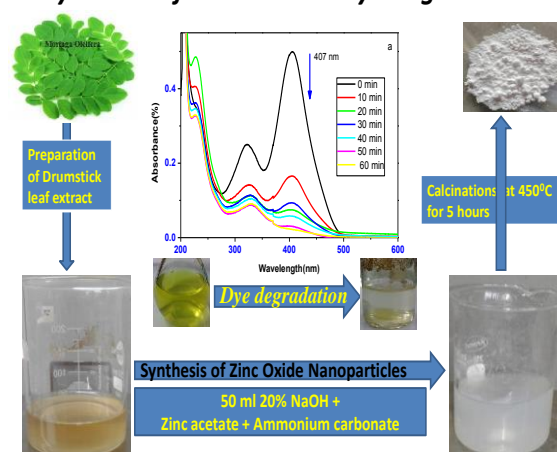


Figure 1. Various steps of ZnONPs synthesis.

$$\text{Percentage of dye degradation,} \\ = \frac{(A_0 - A_t)}{A_0} \times 100\%$$

where,  $A_0$  is the initial dye absorbance and  $A_t$  is the dye absorbance at time  $t$ .

## 2.7. In Vitro Antimicrobial Activity

Antibacterial activity of the ZnONPs was tested by Agar Cup Method [32] for qualitative antimicrobial screening. Two test microorganisms (*Bacillus subtilis* and *E. coli*) were used for this analysis. In this technique, sterilized Nutrient Agar Plates were prepared and to it, the test organism i.e. *Bacillus subtilis* and *E. coli* were swabbed uniformly throughout the nutrient agar medium with the help of sterile cotton swab. Then with the help of Cork Borer, wells were prepared on the surface of nutrient agar plates. Then the prepared ZnO nanoparticles were placed in the wells of the plate and the nutrient agar plates were incubated at 37 $^{\circ}$ C for 24h. At the end of the incubation period, the plates were examined for evidence of zone of inhibition which appeared as a clear area around the wells and was measured in cm unit.

## 3. RESULTS AND DISCUSSION

The present study reports the use of dried leaf for the synthesis of nanoparticles which are free from external stabilizing and accelerating agents and does not require

continuous agitation. The appearance of white precipitate is a clear indication of the formation of ZnONPs formed in the reaction mixture.

### 3.1. UV-VIS Spectra Analysis

Figure 2 shows the absorption spectrum of the synthesized ZnONPs with the absorption peak around 361 nm. It indicates that ZnONPs displays excitation absorption (at 361 nm) due to their large excitation binding energy at room temperature. The sharp bands of zinc colloids were observed at 361 nm, which proves that the zinc ion is efficiently reduced by the *Moringa Oleifera* leaf extract. The wavelength of 361 nm absorption peak confirms the occurrence of blue-shifted absorption spectrum with respect to the bulk value (377 nm) of the ZnONPs, due to the quantum confinement effect, which is in good agreement with the previous report [33].

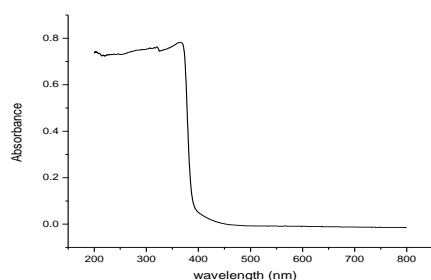


**Figure 2.** UV-Visible of ZnO nanoparticle.

### 3.2. FTIR Analysis

FTIR measurement (Figure 3) was carried out to identify the possible biomolecules in *Moringa Oleifera* leaf extract responsible for capping leading to efficient stabilization of the ZnONPs. The FTIR spectra shows the presence of bonds due to -OH stretching frequency around  $3444\text{ cm}^{-1}$ . However, peaks at  $2918\text{ cm}^{-1}$  and  $2852\text{ cm}^{-1}$  are attributed to the asymmetric and symmetric stretching vibrations of -CH<sub>2</sub> group respectively. The peak at  $1614\text{ cm}^{-1}$  results from the stretching bands of C=O functional groups (Rastogi and Arunachalam, 2011). The peak at around  $1383\text{ cm}^{-1}$  present in ZnO signified amide band of the random coil of protein [34]. The peak at  $682\text{ cm}^{-1}$  indicates the stretching vibrations

of ZnO nanoparticle which is consistent with that reported earlier [35]. The region between  $400$  and  $600\text{ cm}^{-1}$  is assigned for metal-oxygen bond. In addition to the absorption bands of the biomolecules used as reduction and stabilization (capping agents), the absorption peak at  $440\text{ cm}^{-1}$  indicate the presence of ZnONPs [36].

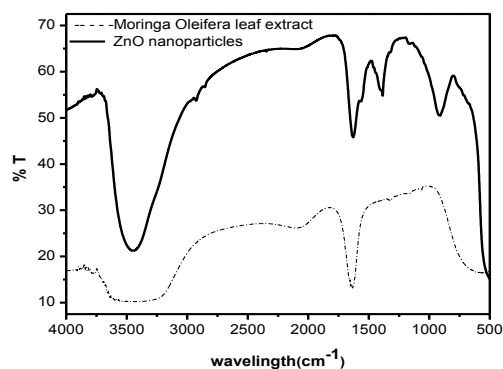


**Figure 3.** FTIR spectra of leaf extract of *Moringa Oleifera* (---) and Synthesized ZnO Nanoparticles (---).

### 3.3. XRD Analysis of ZnO Nanoparticles

XRD patterns of synthesized ZnONPs reflect that all the diffraction peaks of ZnONPs matches with the standard ZnONPs data. Diffraction peaks (Figure 4) of XRD are very well matched with the hexagonal wurtzite structure by comparison with the data from JCPDS card No. 89-1397 [37]. The sharp and intense peaks in Fig. 4 indicate that the samples are highly crystalline. The pattern can be indexed for diffractions from the (1 0 0), (0 0 2), (1 0 1), (1 0 2), (1 1 0), (1 0 3), (2 0 0), (1 1 2) and (2 0 1) planes. No other diffraction peaks corresponding to impurity is found confirming the high purity of the synthesized products. From the XRD data, it was found that the peaks are broad; suggesting that the crystallites have sizes in the nanometer range and the diameter (D) was calculated using Debye-Scherrer's formula

$$D = \frac{K\lambda}{\beta \cos\theta}$$

Where K is the Scherrer constant,  $\lambda$  is the X-ray wavelength,  $\beta$  is the peak width of half maximum, and  $\theta$  is the Bragg

diffraction angle [38]. The average crystallite size of zinc oxide is estimated by XRD data and it was obtained around 52nm.

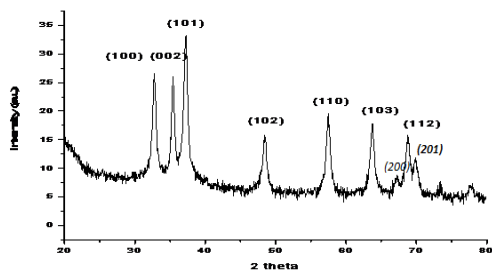


**Figure 4.** XRD patterns of ZnO nanoparticles.

### 3.4. SEM Analysis

After the substantiation of XRD results the sample was further preceded for the SEM study. The size, shape and surface morphology of the ZnONPs is clearly indicated by SEM image as shown in Figure 5. Detailed structural characterizations demonstrate that the synthesized products are spherical and crystalline in structure and their diameters were about 52nm.

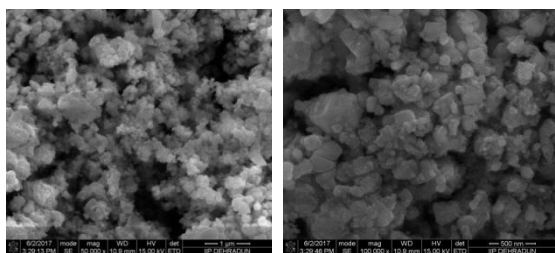


**Figure 5.** SEM images of green synthesized ZnO nanoparticles.

### 3.5 Photocatalytic Activity of ZnONPs under Visible Light

Photo-catalytic degradation of titan yellow dye was performed using green synthesized ZnONPs in different time intervals are shown in Figure 6. Titan yellow is an aromatic heterocyclic chemical compound. The spectrum of the titan yellow solution (Figure 6) in aqueous medium shows characteristics peaks at 226, 321 and 407 nm.

Then after several time intervals in the presence of ZnONPs suspension the absorbance decreases from 407 nm in presence of visible light illumination is

probably due to the breakdown of the chromospheres.

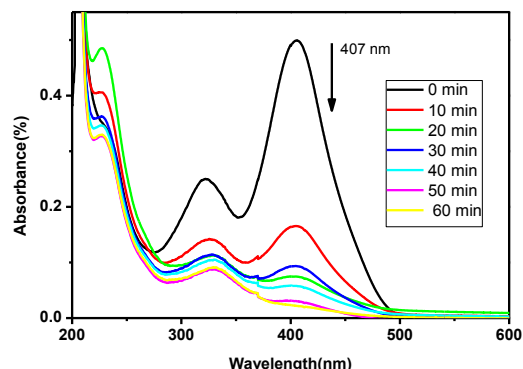


**Figure 6.** Adsorption changes of Titan yellow aqueous solution at room temperature in the presence of ZnO nanoparticles obtained under visible light irradiation.

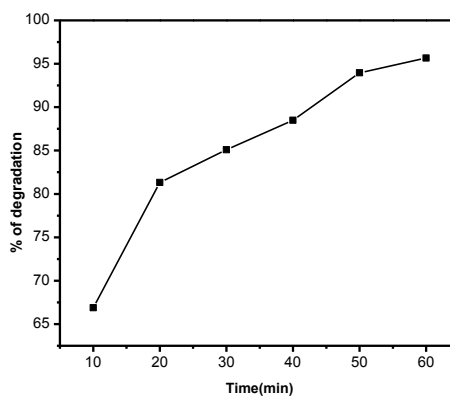


**Figure 7.** Photo degradation efficiency of titan yellow dye with time.

The photo-catalytic properties of the synthesized ZnONPs are well known and it depends on several factors like size, morphology, surface area and electronic state of metal of that particular nanoparticles. The self-degradation of titan yellow dye in presence of visible light was negligible in the absence of photo-catalyst but in presence of our synthesized nanoparticles the dye depredate almost 96%. It was previously reported that particle sizes play important role as photocatalytic degradation, the photo-catalytic activity decreases due to decrease in surface area [39]. The decreases of absorbance of titan yellow dye solution to

presence of ZnONPs proved that the synthesized nanoparticles have significant photo degradation ability.

It can be seen from Figure 7 that the degradation efficiency increases over time. Table 1 shows the comparison of the degradation (%) of different dye using ZnONPs in the various range of dye

solution pH. From the table it can be concluded that our synthesized nanoparticles show excellent degradation at minimum time range. The color change of dye solution is shown in Figure 1 (inside picture).

**Table 1.** Effect of catalyst loading on the photo catalytic degradation of various dyes.

| Photo-catalyst | Dye degraded        | Irradiating/time | Range of solution pH | % of Degradation | References                 |
|----------------|---------------------|------------------|----------------------|------------------|----------------------------|
| ZnO            | Methyl Orange       | 120 min          | 2.0–12.0             | ~60%             | Comparelli et al. [40]     |
| ZnO            | Alizarin Yellow     | 40 min           | 5.0–12.2             | ~80%             | Hayat et al. [41]          |
| ZnO            | Methyl Green        | 1440 min         | 4.0–10.0             | 100%             | Mai et al. [42]            |
| ZnO            | Rhodamine B         | 100 min          | 4.5–10.5             | 100%             | Zhai et al. [43]           |
| ZnO            | Methyl Red          | 120 min          | 2.0–12.0             | ~80%             | Comparelli et al. [40]     |
| ZnO            | Remazol Red F3B     | 60 min           | 6.0–10.0             | ~98%             | Akyol and Bayramoglu [44]  |
| ZnO            | Eosin Y             | 120min           | 2.0–12.0             | 74%              | Chakrabarti and Dutta [45] |
| ZnO            | C.I. Acid Yellow 23 | 60min            | 2.28–9.52            | 93%              | Behnajady et al. [46]      |
| ZnO            | Methyl Orange       | 120min           | 2.0–12.0             | ~95%             | Chen et al. [47]           |
| ZnO            | Methylene Blue      | 120mi            | 4.5–10.5             | 76%              | Chakrabarti and Dutta [45] |
| ZnO            | Congo Red           | 120min           | 6.0–11.0             | 97%              | Annadurai et al. [48]      |
| ZnO            | Reactive Black 5    | 60 min           | 3.0 –11.0            | ~60%             | Amisha et al. [49]         |
| ZnO            | Basic Blue 11       | 1440 min         | 1.0–7.0              | ~98%             | Lu et al. [50]             |
| ZnO            | Titan yellow        | 60 min           | 2.0–12.0             | ~96%             | In our work                |

### 3.6 Antibacterial Activity

The anti-bacterial activity of the ZnO nanoparticles were tested for gram positive and gram negative bacteria. The results are shown in Table: 2 clearly represent the excellent anti-bacterial activity of ZnO nanoparticles against *Bacillus subtilis* (gram positive) and *E. coli* (gram negative). The experimental outcomes undeniably suggest an effective growth inhibitory activity of the nanoparticles upon both the microorganisms and strong activity alongside *Bacillus subtilis* and *E. coli*.

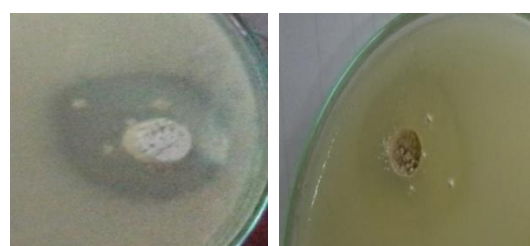


**Figure 8.** Zone of inhibition of ZnO nanoparticles against *Bacillus subtilis* and *E. coli*.

**Table 2.** Diameters of inhibition zone (cm) of ZnONPs against bacterial species.

| Samples | Zone of inhibition (cm)  |                         |
|---------|--------------------------|-------------------------|
|         | <i>Bacillus subtilis</i> | <i>Escherichia coli</i> |
| ZnONPs  | 3.5 cm                   | 3.3 cm                  |

#### 4. CONCLUSION

In this work we have synthesized ZnO-NPs by a very simple and efficient precipitation method using *Moringa Oleifera* leaf extract as natural precursor. The main advantage of this synthesis is its simple and cost-effective synthetic route. In this way we can extract *Moringa Oleifera* leaf for large scale production of ZnONPs. The formation of ZnO nanoparticles was confirmed by FE-SEM, and XRD analysis. The synthesized nanoparticles are very much active in degrading titan yellow dye solution and catalyze the decolonization in presence of visible light illumination. The synthesized ZnO-NPs were studied for antibacterial activities against pathogenic

bacteria like *Bacillus subtilis* and *E. coli* at a very low concentration. It may be concluded from study of all the above factors, that this procedure is an efficient method of preparation of nanoparticles.

#### ACKNOWLEDGEMENT

The authors are thankful to the Sidho-Kanho-Birsha University, Purulia and Department of Higher Education, Science & Technology and Biotechnology, Government of West Bengal, India for financial support. The authors are also thankful to Dr. R. Bal, Department of Conversion & Catalysis Division, CSIR -Indian Institute of Petroleum, Dehradun, India.

#### REFERENCES

1. Cui, Y., Lieber, C. M. (2001). "Functional nanoscale electronic devices assembled using nanowire blocks", *Science.*, 29: 851-853.
2. Jones, M. R. (2011). "Templated Techniques for the Synthesis and Assembly of Plasmonic Nanostructures", *Chemical Reviews.*, 111: 3736-3827.
3. Bala, N., Saha, S., Chakraborty, M., Maiti, M., Das, S., Basu, R., Nandy, P. (2015). "Green synthesis of zinc oxide nanoparticles using *Hibiscus subdariffa* leaf extract: effect of temperature on synthesis, anti-bacterial activity and anti-diabetic activity", *RSC Adv.*, 5: 4993-5003.
4. Roduner, E. (2006). "Size matters: why nanomaterials are different", *Chemical Society Reviews.*, 35: 583-592.
5. Irvani, S. (2013). "Green synthesis of metal nanoparticles using plants", *Green Chemistry.*, 13: 2638-2650.
6. Mohamed, R. M., Mkhallid, I. A., Baeissa, E. S., Al-Rayyani, M. A. (2012). "Photocatalytic Degradation of Methylene Blue by Fe/ZnO/SiO<sub>2</sub> Nanoparticles under Visiblelight", *Journal of Nanotechnology.*, 2012-2016.
7. Shankar, S. S., Ahmad, A., Sastry, M. (2003). "Geranium leaf assisted biosynthesis of silver nanoparticles", *Biotechnol. Prog.*, 19: 1627.
8. Shankar, S. S., Rai, A., Ahmad, A., Sastry, M. (2004). "Rapid synthesis of Au, Ag, and bimetallic Au core-Ag shell nanoparticles using Neem (*Azadirachta indica*) leaf broth", *J. Colloid Interf. Sci.*, 75: 496.
9. Shankar, S. S., Rai, A., Ahmad, A., Sastry, M. (2005). "Controlling the Optical Properties of Lemongrass Extract Synthesized Gold Nanotriangles and Potential Application in Infrared-Absorbing Optical Coatings", *Chem. Mater.*, 17: 566.
10. Chandran, S. P., Chaudhary, M., Pasricha, R., Ahmad, A., Sastry, M. (2006). "Synthesis of gold nanotriangles and silver nanoparticles using Aloe vera plant extract", *Biotechnol. Prog.*, 22: 577.
11. Huang, J., Li, Q., Sun, D., Lu, Y., Su, Y., Yang, X., Wang, H., Wang, Y., Shao, W., He, N., Hong, J., Chen, C. (2007). "Green Synthesis and Characterization of Gold Nanoparticles Using Onion (*Allium cepa*) Extract", *Nanotechnology.*, 18: 105.
12. Rasmussen, W. J., Martinez, E., Louka, P., Wingett, G. D. (2010). "Zinc oxide nanoparticles for selective destruction of tumor cells and potential for drug delivery applications", *Expert Opin. Drug Delivery.*, 7: 1063-1077.
13. Yoon, H. S., Kim, J. D. (2006). "Fabrication and Characterization of ZnO Films for Biological Sensor Application of FPW Device". *Applications of ferroelectrics.*, 15th IEEE international symposium., 3: 322-325.
14. Xiong, M. H. (2013). "ZnO Nanoparticles Applied to Bioimaging and Drug Delivery", *Adv. Mater.*, 25: 5329-5335.
15. Nie, L., Gao, L., Feng, P., Zhang, J. (2006). "Three-Dimensional Functionalized Tetrapod like ZnO Nanostructures for Plasmid DNA Delivery", *Small.*, 2: 621-625.
16. Apperlot, G., Lipovsky, A., Dror, R., Perkas, N. (2009). "Enhanced antibacterial activity of nanocrystalline ZnO due to increased ROS-mediated cell injury", *Adv. Funct. Mater.*, 19: 842-852.
17. Sharma, D., Rajputa, J., Kaitha, S. B., Kaur, M. (2010). "Synthesis of ZnO nanoparticles and study of their antibacterial and antifungal properties", *Thin Solid Films.*, 519: 1224-1229.

18. Nair, S. (2009). "Role of size scale of ZnO nanoparticles and microparticles on toxicity toward bacteria and osteoblast cancer cells", *J. Mater. Sci.: Mater. Med.*, 20: 235–241.
19. Kirthi, V. A., Rahuman, A. A., Rajakumar, G., Marimuthu, S. (2011). "Acaricidal, pediculocidal and larvicidal activity of synthesized ZnO nanoparticles using wet chemical route against blood feeding parasites", *Parasitol. Res.*, 109: 461–472.
20. Alkaladi, A., Abdelazim, M. A., Afifi, M. (2014). "Antidiabetic Activity of Zinc Oxide and Silver Nanoparticles on Streptozotocin-Induced Diabetic Rats", *Int. J. Mol. Sci.*, 15: 2015–2023.
21. Jiménez-Ferrer, E., Alarcón-Alonso, J., Aguilar-Rojas, A. (2012). "Zamilpa A Diuretic effect of compounds from *Hibiscus sabdariffa* by modulation of the aldosterone activity", *Planta. Med.*, 78: 1893-98.
22. Sharaf, A. (1962). "The pharmacological characteristics of *Hibiscus sabdariffa* L". *Planta. Med.*, 10: 48–52.
23. Salleh, N., Runnie, I., Roach, D., Mohamed, S. (2002). "Inhibition of low-density lipoprotein oxidation and upregulation of low-density lipoprotein receptor in HepG2 cells by tropical plant extracts", *J. Agric. Food. Chem.*, 50: 3693-3697.
24. Lin, H. H., Chen, H. J., Wang, J. C. (2011). "Chemopreventive properties and molecular mechanisms of the bioactive compounds in *Hibiscus sabdariffa* Linne. Curr", *Med. Chem.*, 18: 1245-54.
25. Ajiboye, O. T., Salawu, A. N., Yakubu, Y. M., Oladiji, T. (2011). "A Antioxidant and drug detoxification potentials of *Hibiscus sabdariffa* anthocyanin extract. Drug", *Chem. Toxicol.*, 34: 109-115.
26. He, J., Lindstroem, H., Hagfeldt, A., Lindquist, S. E. (1999). "Dye-sensitized nanostructured p-type nickel oxide film as a photocathode for a solar cell", *J. Phys. Chem. B.*, 103: 8940-8943.
27. Ghosh, M., Biswas, K., Sundaresan, A., Rao, C. N. R. (2006). "MnO and NiO nanoparticles: Synthesis and magnetic properties", *J. Mater Chem.*, 16: 106-111.
28. Tao, F., Saen, Y., Wang, L. (2012). "Controlled fabrication of flower-like Nickel oxide Hierarchical structure and their application in water treatment", *Molecules.*, 17: 703-715.
29. Karunakaran, C., Gomathisankar, P., Manikandan, G. (2010). "Structural and Optical Properties of Cu<sup>2+</sup> + Ce<sup>3+</sup> Co-Doped ZnO by Solution Combustion Method", *Material Chemistry and Physics.*, 123: 585-94.
30. Mehran, M., Sheikhshoaei, F., Sheikhshoaei, I. (2017). "Effect of Nano-Textured Silicon Substrate on the Synthesize of Metal Oxides Nanostructures", *Int. J. Nanosci. Nanotechnol.*, Vol.,13(3): 265-274.
31. Khaleghi, M., Madani, M., Parsia, P. (2017). "Biosynthesis Characteristic of Silver Nanoparticles Produced by Mine Soil Bacteria Isolation, Kerman, Iran", *Int. J. Nanosci. Nanotechnol.*, Vol.,13: 307-313.
32. Bauer, W. A., Kirby, M. M. W., Sherris, C. J., Truck, M. Am. (1996). "Antibiotic susceptibility testing by a standardized single disk method", *J. Clin. Pathol.*, 45: 493-6.
33. Elumalai, K., Velmurugan, S., Ravi, S., Kathiravan, V., Ashokkumar, S. (2015), "Green synthesis of zinc oxide nanoparticles using *Moringa oleifera* leaf extract and evaluation of its antimicrobial activity", *Spectrochimica Acta Part A: Molecular and Biomolecular Spectroscopy.*, 143: 158–164.
34. Cai, S., Sing, R. B. (2004). "A distinct utility of the amide III infrared band for secondary structure estimation of aqueous protein solutions using partial least squares methods", *Biochemistry.*, 43: 2541–2549.
35. Ravichandrika, K. (2012). "Synthesis, Characterization and Antibacterial Activity Of ZnO Nanoparticles", *International Journal Of Pharmacy And Pharmaceutical Sciences.*, 4: 336- 338,
36. Varghese, E., George, M., (2015). "Green synthesis of zinc oxide nanoparticles", *International Journal of Advance Research In Science And Engineering.*, 4: 01.
37. Joel, C., Sheik, M., Badhusha, M., (2016). "Green synthesis of ZnO Nanoparticles using *Phyllanthus emblica* Stem extract and their Antibacterial activity", *Der Pharmacia Lettre.*, 8: 218-223.
38. Navaza, J., Silva, A. M. (1979). "A geometrical-approach to solving crystal structures", *Acta Crystallographica section A.*, 35: 266-275.
39. Wei, W., Jiang, X., Lu, L., Yang, X., Wang, X. (2009). "Study on the catalytic effect of NiO nanoparticles on the thermal decomposition of TEGDN/NC propellant", *J. Hazard Mater.*, 168: 838-842.
40. Comparelli, R., Fanizza, E., Curri, L. M., Cozzoli, D. P., Mascolo, G., Agostiano, A. (2005). "UV induced photocatalytic degradation of azo dyes by organic-capped ZnO nanocrystals immobilized onto substrates", *Appl. Catal. B: Environ.*, 60: 1–11.
41. Hayat, K., Gondal, A. M., Khaled, M. M., Ahmed, S. (2010). "Kinetic study of laser-induced photocatalytic degradation of dye (alizarin yellow) from wastewater using nanostructured ZnO", *J. Environ. Sci. Health, Part A.*, 45: 1413–1420.
42. Mai, D. F., Chen, C. C., Chen, L. J., Liu, C. S. (2008). "Photodegradation of methyl green using visible irradiation in ZnO suspensions determination of the reaction pathway and identification, of intermediates by a high-performance liquid chromatography–photodiode array–electrospray ionization mass spectrometry method", *J. Chromatogr. A.*, 1189: 355–365.
43. Zhai, J., Tao, X., Pu, Y., Zeng, F. X., Chen, F. X. (2010). "Core/shell structured ZnO/SiO<sub>2</sub> nanoparticles: Preparation, characterization and photocatalytic property", *Appl. Surf. Sci.*, 257: 393–397.
44. Akyol, A., Bayramoglu, M. (2005). "Photocatalytic degradation of Remazol Red F3B using ZnO catalyst", *J. Hazard. Mater.*, 124: 241–246.

45. Chakrabarti, S., Dutta, K. B. (2004). "Photocatalytic degradation of model textile dyes in wastewater using ZnO as semiconductor catalyst", *J. Hazard. Mater.*, 112: 269–278.
46. Behnajady, A. M., Modirshahla, N., Hamzavi, R. (2006). "Kinetic study on photocatalytic degradation of CI Acid Yellow 23 by ZnO photocatalyst", *J. Hazard. Mater.*, 133: 226–232.
47. Chen, C. C., Liu, F. J., Liu, P., Yu, H. B. (2011). "Investigation of photocatalytic degradation of methyl orange by using nano-sized ZnO catalysts", *Adv. Chem. Eng. Sci.*, 1: 9–14.
48. Annadurai, G., Sivakumar, T., Rajesh, Babu. S. (2000). "Photocatalytic decolorization of congo red over ZnO powder using Box-Behnken design of experiments", *Bioprocess Biosyst. Eng.*, 23: 167–173.
49. Amisha, S., Selvam, K., Sobana, N., Swaminathan, M. (2008). "Photomineralisation of Reactive Black 5 with ZnO using solar and UV-A light", *J. Korean Chem. Soc.*, 52: 66–72.
50. Lu, S. C., Wu, T. Y., Mai, F., Chung, S. W., Wu, W. C., Lin, Y. W., Chen, C. C. (2009). "Degradation efficiencies and mechanisms of the ZnO-mediated photocatalytic degradation of Basic Blue 11 under visible light irradiation", *J. Mol. Catal. A: Chem.*, 310: 159–165.